

Cryo-TEM and SANS Microstructural Study of Pluronic Polymer Solutions

Kell Mortensen[†] and Yeshayahu Talmon^{*,‡}

Department of Solid State Physics, Risø National Laboratory, DK-4000 Roskilde, Denmark, and Department of Chemical Engineering, Technion—Israel Institute of Technology, Haifa 32000, Israel

Received April 6, 1995; Revised Manuscript Received September 18, 1995[®]

ABSTRACT: Cryogenic temperature transmission electron microscopy (cryo-TEM) and small-angle neutron scattering (SANS) were combined to give complete microstructural characterization of aqueous solutions of Pluronic F127, an (EO)₉₉(PO)₆₅(EO)₉₉ triblock copolymer. The images of vitrified specimens observed by cryo-TEM provided direct information about the building blocks of these systems, i.e., spheroidal micelles. This confirmed the structural model obtained from analysis of SANS data, which, in addition, provide quantitative information about the system. Occasionally spheroidal micelles were pressed closer to each other during specimen preparation, thus giving rise locally to higher concentration. The cubic phase that was thus formed was directly imaged. The existence of this lyotropic liquid crystalline phase was confirmed by SANS of an originally higher concentration solution. When exposed to shear, the polycrystalline phase transforms into a monodomain crystal with cubic symmetry. The system was also used to demonstrate the potential of selective electron beam radiolysis to enhance contrast in radiation-sensitive, inherently low-contrast systems.

I. Introduction

Complete structural characterization of a complex fluid requires accurate direct information on the structural elements of which the system is made up and quantitative information on the sizes in the system. The most effective experimental approach combines cryogenic temperature electron microscopy (cryo-TEM) with indirect techniques such as nuclear magnetic resonance (NMR), small-angle neutron scattering (SANS), or small-angle X-ray scattering (SAXS). This approach has been demonstrated, for example, in the study of lyotropic cubic phases,¹ polymer/surfactant interactions,² and surfactant lamellar phases.^{3,4}

Surfactant systems based on amphiphilic block copolymers have recently attracted great interest, both as a result of their novel physical characteristics and due to their technological possibilities. The applications include utilities as cleaning agents, in products such as cosmetics, shampoos, and lotions, and as dispersants for printing inks, paints, and coatings. The Pluronics, triblock copolymers of poly(ethylene oxide) and poly(propylene oxide) blocks, have in particular been the subject of intense research.^{5–14}

Scattering experiments have shown that these block copolymers typically associate into aggregates of spherical micelles^{6,10,15} but also into rodlike micelles and possibly layered forms. The structure of the aggregates depends on both the specific molecular design¹⁵ and thermodynamic parameters.^{6,10,16} In the high-concentration regimes, micellar aggregates constitute the basis for a variety of crystalline mesophases.^{8,9} Thus, in some respects these block copolymer surfactants behave as typical low molecular weight amphiphiles. There are important differences, though: triblock copolymer systems as block copolymer systems in general have, for example, no clear distinction between lyotropic and thermotropic phase behavior.

In this paper we present a first account of applying both SANS and cryo-TEM to the microstructural characterization of aqueous solutions of a Pluronic polymer, (EO)₉₉(PO)₆₅(EO)₉₉, known also as F127. Other aspects of the characterization of F127 had been previously published, e.g., refs 5, 12, 17, and 18.

II. Materials and Methods

A. Materials. The triblock copolymer, poly(ethylene oxide)–poly(propylene oxide)–poly(ethylene oxide), [OCH₂CH₂]₉₉–H[OCH₂CH(CH₃)]₆₅[OCH₂CH₂]₉₉ or EO₉₉PO₆₅EO₉₉ (or PEO–PPO–PEO), designated F127, was obtained from BASF Corp., Wyandotte, USA, and was used without further purification. The triblock copolymer was dissolved in D₂O at 5 °C, where it forms a homogeneous solution. Deuterium oxide, D₂O, was used to obtain good contrast and low background in the neutron scattering experiments. For TEM specimens the polymer was dissolved in H₂O. The concentrations of the solutions discussed below are all given in weight percent (wt %).

B. Cryo-TEM. Specimens for electron microscopy were prepared in a controlled environment vitrification system (CEVS) to ensure fixed temperature and to avoid water loss from the solution during sample preparation. The specimens were prepared as thin liquid films, less than 0.25 μm thick, on perforated polymer/carbon films and quenched into liquid ethane at its freezing point. The technique and apparatus were described in detail by Bellare et al.¹⁹ The technique leads to vitrified specimens; i.e., the water does not undergo crystallization during thermal fixation. This way, component segregation and rearrangement are prevented, and the original fluid microstructure is preserved. The vitrified specimens were stored under liquid nitrogen, and subsequently transferred to the electron microscope (JEOL 2000FX), using a Gatan 626 cryoholder and its “workstation”. Imaging was carried out at a temperature of about –170 °C and 100 kV acceleration voltage. Low doses of less than 10 e/Å² were normally used for imaging, except when we applied selective electron beam etching (see below). We used Kodak SO-163 electron imaging film, developed for maximum electron speed.

C. Small-Angle Neutron Scattering. Small-angle neutron scattering experiments were performed using the Rosø SANS facility. The dilute samples were mounted in sealed quartz containers (Suprasil from Hellma, FRG), with 2 mm flight path. The 20 wt % sample was in addition studied when mounted in a sealed Couette type shear cell.²⁰

* To whom correspondence should be addressed.

[†] Risø National Laboratory.

[‡] Technion—Israel Institute of Technology.

[®] Abstract published in *Advance ACS Abstracts*, November 1, 1995.

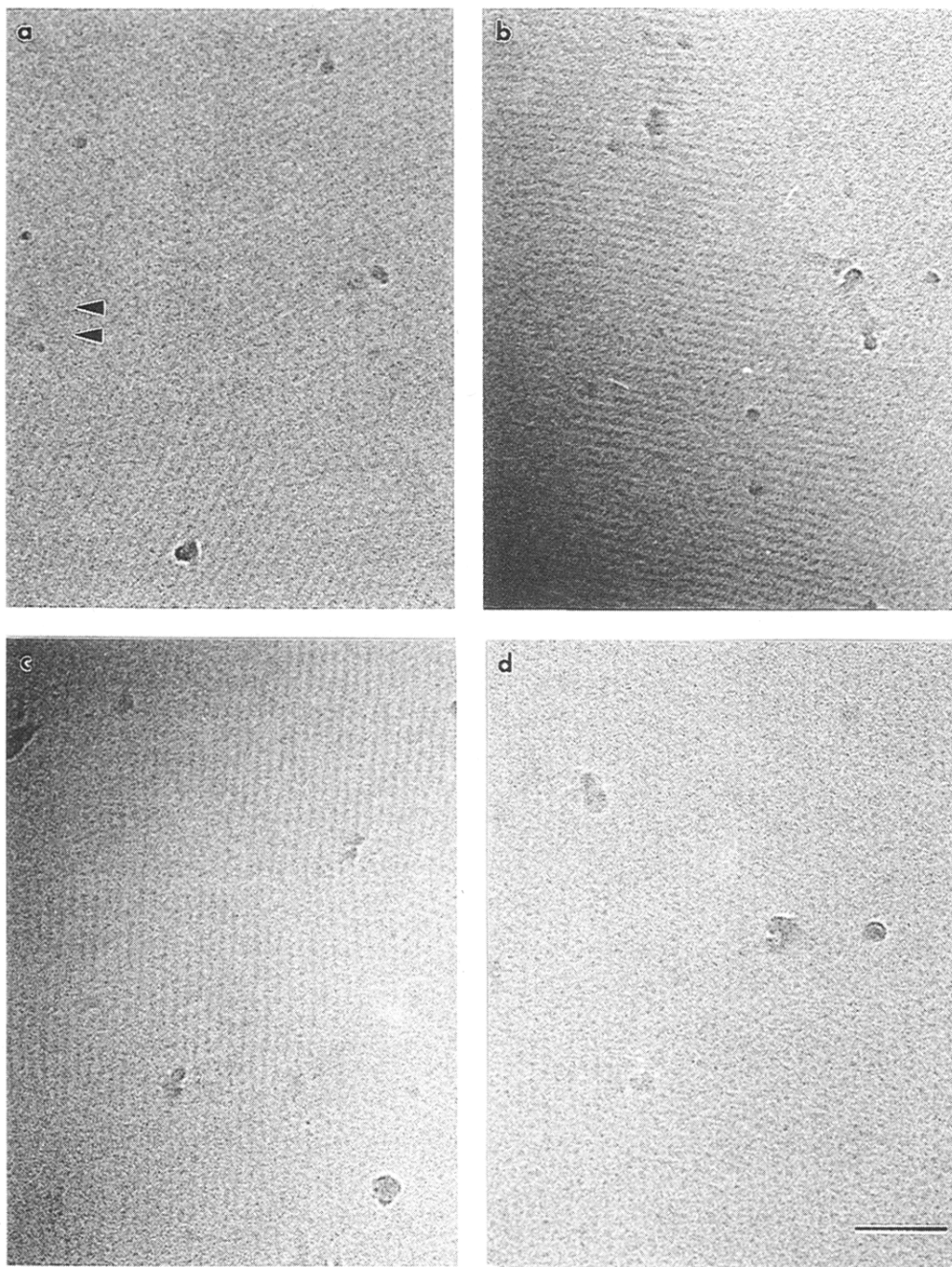


Figure 1. Vitrified specimens of 11.7% Pluronic F127 in water: (a) micelles, arranged in parallel lines; in thinner areas (arrowheads) no micelles are seen; (b) an area of the same specimens, with a steep thickness gradient; (c) "micellar lattice fringes" with very long-range order; (d) a thin area with dark dots, approximately 5–7 nm in diameter, that in all probability are the micellar hydrophobic cores of the micelles. Scale bar = 100 nm.

The results presented below were obtained using the combined scattering pattern obtained with neutrons with 3, 5, 9, and 15 Å wavelength, with sample-to-detector distances of 1, 3, and 6 m, giving a total range of scattering vectors $0.002\text{--}0.5\text{ \AA}^{-1}$, where the scattering vector \bar{q} is given by the scattering angle, θ , and the neutron wavelength, λ :

$$|\bar{q}| = q = 4\pi/\lambda \sin(\theta/2)$$

The neutron wavelength resolution was $\Delta\lambda/\lambda = 0.18$, and the neutron beam collimation was determined by the pinhole sizes of 16 and 7 mm diameter at the source and sample positions, respectively, and the collimation length was equal to the sample-to-detector distance. Smearing induced by the wavelength spread, the collimation, and the detector resolution was included in the data analysis discussed below, using Gaussian approximations for the different terms.

The scattering data were corrected for the background arising from either the quartz cell or the Couette cell with D_2O , and from other sources, as measured with the neutron beam blocked by a piece of plastic containing boron at the sample position. The incoherent scattering from H_2O was used to determine deviations from a uniform detector response and to convert the data into absolute units.

The scattering patterns discussed in the present paper are all, except for the 20 wt % sample when sheared in the gel phase, azimuthally isotropic. The data have been reduced, by azimuthally averaging, to the one-dimensional $I(q)$ scattering functions which depend only on the absolute value of \bar{q} . Temperature-dependence neutron scattering data were obtained in both heating and cooling cycles, thereby verifying reproducibility.

III. Results and Discussion

A. Cryo-TEM. Figure 1 shows four different fields of vitrified specimens of 11.7% Pluronic F127 in water. Figure 1a shows a rather thin area. In some areas (arrowheads), no micelles are seen, while in the lower part of the micrograph, one sees micelles, arranged in parallel lines. The latter represent areas where micelles have been pushed together and closely packed by thinning down of the specimen during preparation. This effect had been documented already in early cryo-TEM applications in the study of colloidal systems.²¹ In some cases, this effect may actually be used to our benefit to form high-concentration phases on the grid from a lower concentration phase.¹

Figure 1b shows another area of the same specimen, with a steep thickness gradient. In the thicker (darker) area, individual micelles cannot be distinguished, because the micrograph shows a projection of too many closely packed micelle layers. The observed fringes may have a very long-range order, as demonstrated by Figure 1c. These structures are quite similar to "lattice fringes" seen in high-resolution transmission electron micrographs of crystals. However, in our case the building blocks of these structures are micelles, not atoms. The characteristic periodicity of the fringes is about 14 nm. Of course, measurement accuracy in the TEM without a local built-in calibration standard is rather poor ($\pm 10\%$), a fact that is not always taken into consideration. It must be remembered that in this case the observed long-range order is a result of locally increased concentration during specimen preparation. No such structure was detected by SANS at the given original solution concentration.

Individual micelles of the polymer are difficult to visualize due to the very low contrast between the polymer and water. In fact, poly(ethylene oxide) alone, as free polymer chains, or surfactant micelle-decorated chains, is practically transparent to the electron beam.² Very thin areas of the sample, where one would expect relatively good contrast, contain no micelles at all. In thicker areas, individual micelles are practically invisible. In some cases, however, due to the right combination of specimen thickness and objective lens defocus to enhance phase contrast, single micelles of the polymer are visualized. An example is given in Figure 1d. The dark dots, approximately 5–7 nm in diameter, are in all probability the micellar hydrophobic cores of the micelles. The PEO chains, which are much less densely packed, are transparent to the beam, as explained above.

The problem of low inherent contrast may be alleviated to some extent, as we discovered, by selective electron beam etching. This process, shown in Figure 2, is somewhat similar to selective radiolysis, which we used to study two-component polymer latex systems.^{22,23} Figure 2a is micrograph of a thick area of a vitrified 11.7% aqueous solution of F127 in water. Very little detail of the suspended aggregates is seen in this low-dose micrography, where radiation damage was kept at minimum. Only in a few areas one can see faint fringes (arrow), an indication of closely packed micelles. Figure 2b shows the same field of view after about an additional exposure of 100 e/Å². This time, fringes are visible throughout the micrography, including the area marked in Figure 2a. A close inspection reveals that these are indeed the same fringes (arrow), but this time, visualized at much higher contrast. Due to the thickness of the specimen, one can see also areas of two superposed

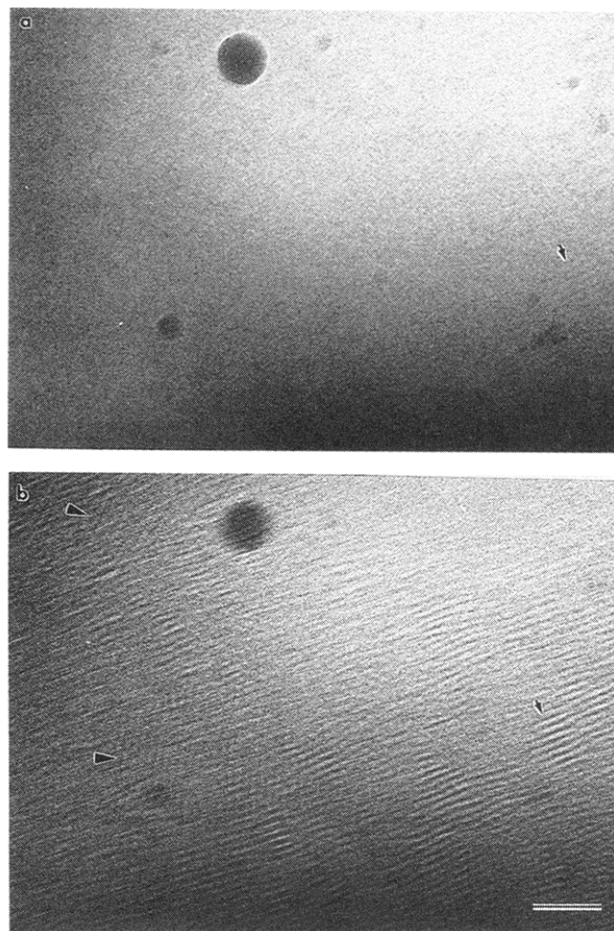


Figure 2. (a) A vitrified 11.7% aqueous solution of F127 in water; only faint fringes (arrow), an indication of closely packed micelles, are observed. (b) The same field of view after about an additional exposure of 100 e/Å²; fringes are visible throughout the micrography, including the area marked in (a). Due to the thickness of the specimen, one can see also areas of two superposed sets of fringes (arrowheads). Scale bar = 100 nm.

sets of fringes (arrowheads). This selective etching is probably the result of very high radiolysis rates at the organic matter/water interface,²⁴ which in this case is the micelle/water interface. Because of the fine segregation of hydrophobic/hydrophilic moieties in this micellar system, the details revealed here by selective electron beam etching are on a much finer scale than those observed in the polymer systems studied in the past.²³

B. SANS. Figures 3–7 show the neutron scattering data for 1, 2, 5, 12, and 20% F127 solutions, as obtained at temperatures in the range 5–95 °C. All the scattering patterns show the following typical characteristics: at low temperatures, the scattering function is relatively weakly dependent on q , and the absolute intensity is low. As the temperature increases, the intensity increases, and the q dependence becomes stronger, revealing aggregation of the copolymer into the micelles observed in cryo-TEM, as discussed above.

At higher temperatures, the scattering functions for the samples with polymer concentrations more than approximately 5% are increasingly dominated by a peak, revealing important spatial correlation between neighboring micelles. The correlation peak becomes significantly more pronounced at high copolymer concentrations. For the 20% copolymer concentration, a slight narrowing of the correlation peak is observed, as a result of micellar ordering on a crystalline lattice. Equivalent

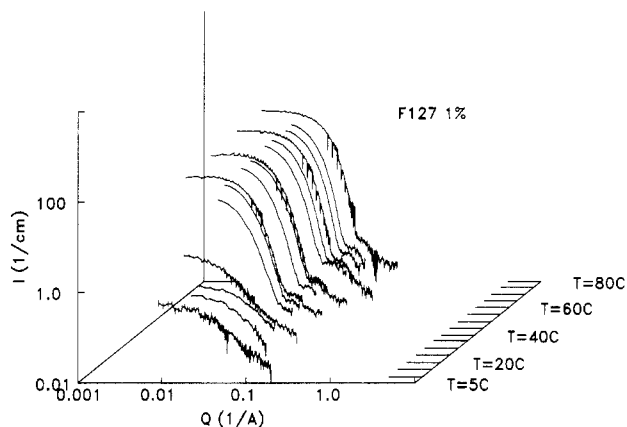


Figure 3. Scattering function I vs Q of 1% F127 in D_2O , as obtained in the 5–80 °C temperature range.

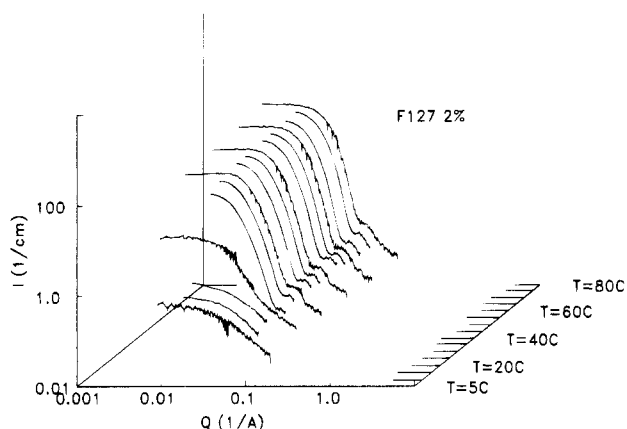


Figure 4. Scattering function I vs Q of 2% F127 in D_2O , in the 5–80 °C temperature range.

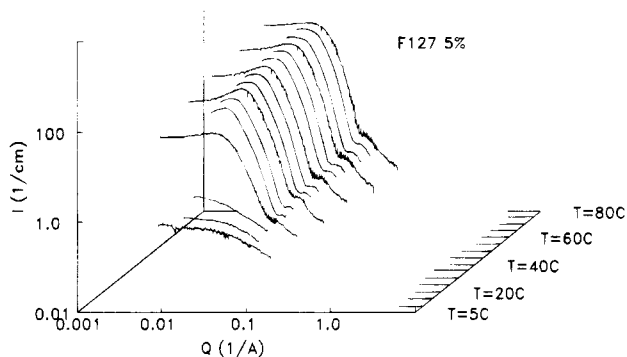


Figure 5. Scattering function I vs Q of 5% F127 in D_2O , as obtained in the 5–80 °C temperature range.

behavior had been observed in related Pluronic systems.^{10,15}

At the highest temperature, $T \geq 95$ °C for 12% and $T \geq 65$ °C for 20%, the scattering function of F127 changes somewhat in character, showing an increasing intensity at the smallest scattering vectors. Similar effects had been seen in other Pluronics, e.g., P85, and had been shown from scattering methods to be a result of a micellar transformation from spherical to rodlike form.¹⁰

The low-temperature neutron scattering patterns of relative small intensity is consistent with the Debye formula for Gaussian chains:¹⁰

$$I(q) \sim (e^{-x} + x - 1)/x^2 + I_{ic} \quad (1)$$

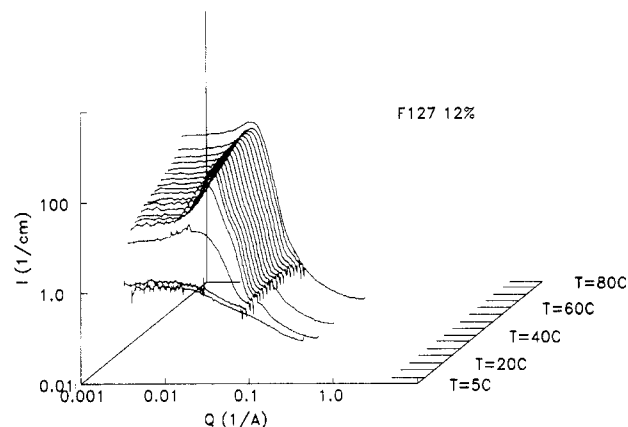


Figure 6. Scattering function I vs Q of 12% F127 in D_2O , as obtained in the 5–95 °C temperature range.

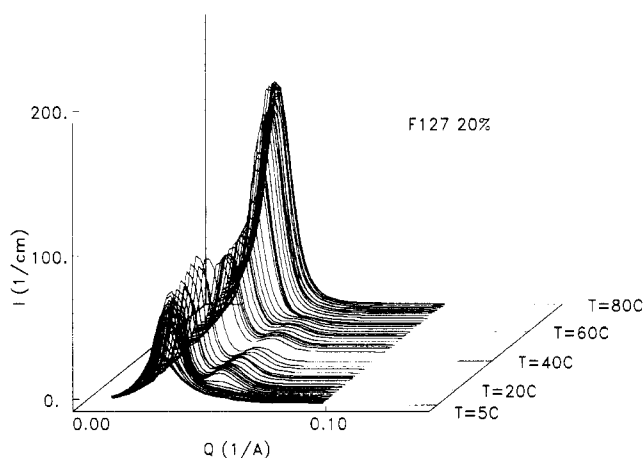


Figure 7. Scattering function I vs Q of 20% F127 in D_2O , as obtained in the 5–80 °C temperature range.

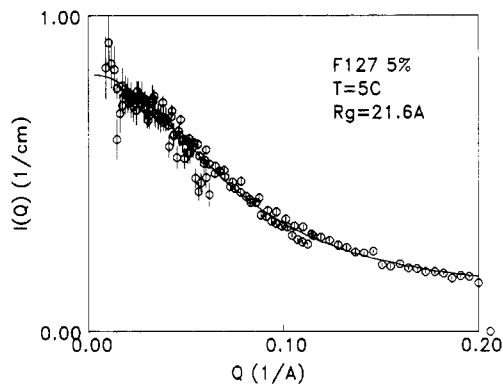


Figure 8. Scattering function I vs Q of 5% F127 in D_2O , as obtained at $T = 5$ °C. The solid line is a least-squares fit of the Debye function to the experimental data, resulting in a polymer radius of gyration $R_g = 21.6$ Å.

where $x = (qR_g)^2$, R_g being the polymer radius of gyration, and I_{ic} represents the incoherent background from the sample. Figure 8 shows the experimental scattering function of 5% F127 obtained $T = 5$ °C. The solid line represents the best fit to the Debye function, including instrumental smearing. The resulting radius of gyration, $R_g = 22$ Å, seems, however, unrealistically small, if the copolymer were really fully dissolved Gaussian chains. Therefore it seems likely that the scattering function is dominated only by the structure of the PEO chains, which obey Gaussian structure, and that the midblock PPO chain effectively has segregated into a small core which scatters only very weakly. Such a structure resemble that of a unimolecular micelle.

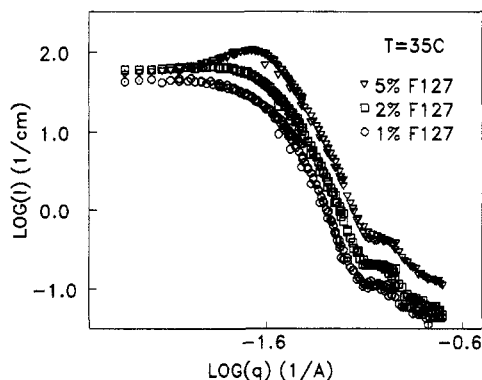


Figure 9. Scattering function I vs Q of 1, 2, and 5% F127 in D_2O , as obtained at $T = 35^\circ C$.

At temperatures close to ambient, the poly(propylene oxide) part of the polymer chain is no longer soluble in water. The resulting amphiphilic character of PEO-PPO-PEO triblock copolymers leads to self-aggregation into spherical micelles. The scattering function of the 1, 2, and 5% samples clearly shows a side maximum as expected from the form factor of dense spherical objects with a sharp interface, with radius R_c :

$$P(q) = \left[\frac{3}{(qR_c)^3} (\sin(qR_c) - qR_c \cos(qR_c)) \right]^2 \quad (2)$$

However, the observed scattering function does not show the q^{-4} approach at large q values, as expected from eq 2. This deviation is attributed to the ethylene oxide subchains dispersed in the water phase, in agreement with a simplified model of the micellar structure with a central dense core of mostly poly(propylene oxide) and an outer corona of hydrated poly(ethylene oxide), effectively grafted onto the surface of the core. As shown in Figure 9, the position of the side maximum is practically unaffected by polymer concentration. The temperature dependence is also rather weak, although some slight increase in micellar size is observed upon raising the temperature.

These findings indicate, in good agreement with the cryo-TEM data discussed above, that the block copolymers form a monodisperse suspension of spherical micelles, characterized by the core size $R_c \sim 50$ Å.

As the temperature or the concentration is increased, the scattering function becomes increasingly dominated by a correlation peak that reveals significant interactions between neighboring micelles (cf. Figures 3–7). In contrast, at the high- q range well beyond the correlation peak, the scattering function remains effectively unchanged, indicating that the changes in the observed scattering pattern reflect primarily the increasing number density of the micelles, whereas the characteristic form of the individual micelle is relatively unaffected by increasing the temperature or the concentration.

Because the micellar dispersion contains identical particles, the scattering function can be written as the product of the form factor of the individual micelle multiplied by the structure factor, $S(q)$, describing intermicellar interferences:²⁵

$$I(q) = \Delta\rho^2 NV^2 P(q) S(q) \quad (3)$$

$\Delta\rho^2$ is the contrast factor and N is the number density of scatterers of volume V . Although it is clear that micelles do not have a sharp surface, as discussed above, we will in the attempt to minimize the number of free

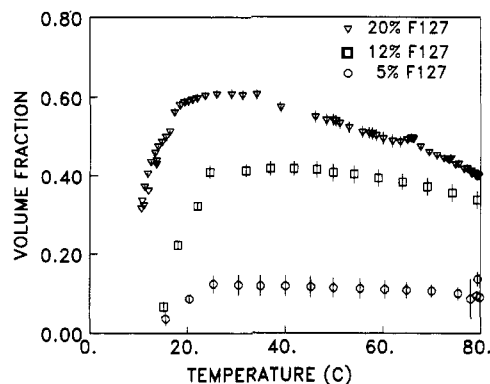


Figure 10. Micellar volume fraction (ϕ) versus temperature for 5, 12, and 20% F127 in D_2O , as obtained by fitting the hard-sphere Percus-Yevick model to the experimental scattering data (Figures 5–7).

variables, analyze the data using the dense sphere approximation for the form factor.

Using the classical Ornstein-Zernike approximation for the spatial correlation fluctuations and the Percus-Yevick approximation for describing the direct correlation between two scattering objects with a hard-sphere nearest-neighbor interaction potential, we can write the structure factor in the analytical form.²⁶

$$S(q) = \frac{1}{1 + 24\phi G(2qR_{hs}\phi)/(2qR_{hs})} \quad (4)$$

G is a trigonometric function of the hard-sphere interaction radius R_{hs} and the hard-sphere volume fraction, ϕ . Thus, by least-squares residual fitting routines, the experimental scattering function can be analyzed in terms of only three parameters characterizing the micellar aggregates: the core radius R_c dominating the form factor $P(q)$, and the hard-sphere interaction parameters R_{hs} and ϕ .

The resulting micellar core radius and interaction radius show similar character as found for related Pluronics.^{10,15} The core radius R_c increases from 50–60 Å at low T to 70–80 Å at the higher temperatures. The interaction radius is of the order of 100–120 Å.

The effective volume fraction occupied by the micelles is the parameter showing the most significant dependence of polymer concentration and temperature. The volume fraction ϕ increases roughly linearly with both polymer concentration and temperature (Figure 10). The high-temperature limit of $\phi = 0.42$ for the 12% sample corresponds to the situation when all polymer molecules have been incorporated into micellar aggregates.

The 20% sample changes from a Newtonian liquid to a solid gel as the temperature is raised above 17 °C. The micellar volume fraction reaches at the same temperature the critical value $\phi_c = 0.53$ for hard-sphere crystallization, thus signifying an inverse melting characteristic, which is typical for the Pluronics.⁸ The characteristic scattering pattern is qualitatively similar to that of other shear-aligned Pluronics,^{8,9} however with more intense higher order reflections. We therefore conclude that the colloidal crystal of F127 is also body centered cubic. With $q = 0.32 \text{ nm}^{-2}$ of the first [110] Bragg reflections, the lattice constant is $a = 28 \text{ nm}$. In comparison, cryo-TEM gives a characteristic interlayer distance of about 14 nm, as discussed above. Thus those cryo-TEM fringes are probably of the [111] planes.

As seen in the cryo-TEM pictures (Figure 1), the domains of more dense micelles are characterized by a

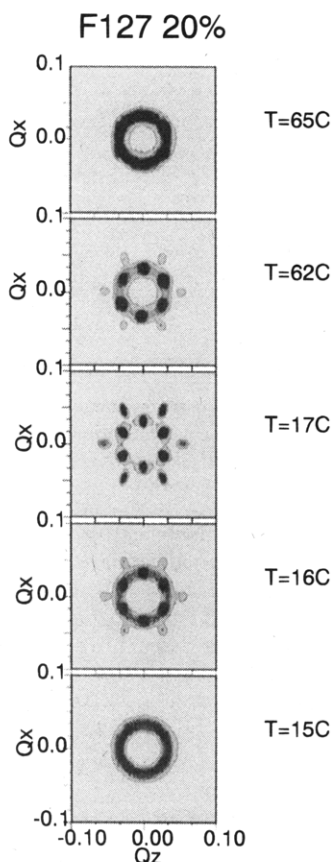


Figure 11. Two-dimensional scattering function of a shear-oriented 20% solution of F127, as obtained at temperatures close to the lower limit ($T = 15^\circ\text{C}$) and upper limit ($T = 65^\circ\text{C}$) of the cubic phase.

high degree of order in the micellar positions. This order is even more evident from scattering experiments performed under shear flow. Using a Couette cell, the shear aligns the $\phi = 0.53$ gel phase into a single domain cubic crystal, as shown in Figure 11. The cubic phase exists up to $T = 65^\circ\text{C}$. Above that temperature, the suspension is liquid, presumably dominated by ellipsoidal or rodlike micelles.

In conclusion, we have shown how the combination of cryo-TEM and SANS leads to a full microstructural characterization of aqueous solutions of a Pluronic, F127. This block copolymer belongs to a class of Pluronics which are dominated by spherical micelles in a wide range of temperature and concentration. Evidence for nonspherical micelles is only found at high temperatures. Polymeric micelles, or more specifically, their hydrophobic cores, can be directly visualized despite the very low inherent contrast in the system.

SANS provides quantitative data, such as the diameter of these micelles. Cryo-TEM can also be applied to visualize the cubic lyotropic phases that are formed by the polymer at higher concentrations. Careful application of selective electron beam etching is potentially a useful tool in enhancing contrast in such systems.

Acknowledgment. Financial support from the Danish Natural Science Research Council is gratefully acknowledged. The microscopy work was done during Y.T.'s stay as a visiting scientist at the Physical Chemistry 1 Department, the University of Lund. Y.T. would like to thank Dr. Raoul Zana of the Institute Charles Sadron, Strasbourg, for suggesting the Pluronics as a candidate micellar system for cryo-TEM.

References and Notes

- (1) Burns, J. L.; Cohen, Y.; Talmon, Y. *J. Phys. Chem.* **1990**, *94*, 5308.
- (2) Süss, D.; Cohen, Y.; Talmon, Y. *Polymer* **1995**, *36*, 1809.
- (3) Regev, O.; Cohen, Y.; Kehat, E.; Talmon, Y. *Zeolites* **1994**, *14*, 314.
- (4) Regev, O.; Kang, C.; Khan, A. *J. Phys. Chem.* **1994**, *98*, 6619.
- (5) Wanka, G.; Hoffmann, H.; Ulbricht, W. *Colloid Polym. Sci.* **1990**, *268*, 101.
- (6) Wanka, G.; Hoffmann, H.; Ulbricht, W. *Macromolecules* **1994**, *27*, 4145.
- (7) Brown, W.; Schillén, K.; Almgren, M.; Hvidt, S.; Bahadur, P. *J. Phys. Chem.* **1991**, *95*, 1850.
- (8) Mortensen, K.; Brown, W.; Norden, B. *Phys. Rev. Lett.* **1992**, *68*, 2340.
- (9) Mortensen, K. *Europhys. Lett.* **1992**, *19*, 599.
- (10) Mortensen, K.; Pedersen, J. S. *Macromolecules* **1993**, *26*, 805.
- (11) Wu, G.; Zhou, Z.; Chu, B. *Macromolecules* **1993**, *26*, 2117.
- (12) Yu, G.-E.; Deng, Y.; Dalton, S.; Wang, Q.-G.; Attwood, D.; Booth, C. *J. Chem. Soc., Faraday Trans.* **1992**, *88*, 2537.
- (13) Linse, P.; Malmsten, M. *Macromolecules* **1992**, *25*, 5434.
- (14) Fleischer, G. *J. Phys. Chem.* **1993**, *97*, 517.
- (15) Mortensen, K.; Brown, W. *Macromolecules* **1993**, *26*, 4128.
- (16) Mortensen, K.; Schwahn, D.; Janssen, S. *Phys. Rev. Lett.* **1993**, *71*, 1728.
- (17) Rassing, J.; Attwood, D. *Int. J. Pharm.* **1983**, *13*, 47.
- (18) Malmsten, M.; Lindman, B. *Macromolecules* **1992**, *25*, 5440.
- (19) Bellare, J. R.; Davis, H. T.; Scriven, L. E.; Talmon, Y. *J. Electron Microsc. Tech.* **1988**, *10*, 87.
- (20) Mortensen, K.; Almdal, K.; Bates, F. S.; Koppi, K.; Tirrell, M.; Norden, B. *Physica B* **1995**, *213 + 214*, 685.
- (21) Talmon, Y. *Colloids Surf.* **1986**, *19*, 237.
- (22) Talmon, Y. Electron Beam Radiation Damage to Organic and Biological Cryo-Specimens. In *Cryotechniques in Biological Electron Microscopy*; Steinbrecht, R. A., Zierold, K., Eds.; SpringerVerlag: Berlin, 1987; Chapter 3, pp 64–84.
- (23) Hass-Bar Ilan, A.; Noda, I.; Schechtman, L. A.; Talmon, Y. *Polymer* **1992**, *33*, 2043.
- (24) Talmon, Y. The Study of IPNs by Cryo-TEM Using Radiation-Damage Effects. In *Advances in Interpenetrating Polymer Networks*; Klempner, D., Frisch, K. C., Eds.; Technomic Publishing Co.: Lancaster, PA, 1990; Vol. 2, pp 141–156.
- (25) Guinier, A.; Fournet, G. *Small Angle Scattering of X-Rays*; Wiley: New York, 1955.
- (26) Kinning, D. J.; Thomas, E. L. *Macromolecules* **1984**, *17*, 1712.

MA950472B